Green and Sustainable Chemistry, 2024, 14, 43-65
https://www.scirp.org/journal/gsc
ISSN Online: 2160-696X
ISSN Print: 2160-6951

Optimization and Characterization of Cellulose Extraction from *Grevillea robusta* (Silky Oak) Leaves by Soda-Anthraquinone Pulping Using Response Surface Methodology

Catherine N. Muya[1,2*], John M. Onyari[1], Lydia W. Njenga[1], Joab O. Onyango[2], Wilson M. Gitari[2]

[1]Department of Chemistry, The University of Nairobi, Nairobi, Kenya
[2]School of Chemical and Material Science, The Technical University of Kenya, Nairobi, Kenya
Email: *catherine.muya@tukenya.ac.ke, jonyari@uonbi.ac.ke, lnjenga@uonbi.ac.ke, joab.onyango@tukenya.ac.ke, mugera.gitari@tukenya.ac.ke

How to cite this paper: Muya, C.N., Onyari, J.M., Njenga, L.W., Onyango, J.O. and Gitari, W.M. (2024) Optimization and Characterization of Cellulose Extraction from *Grevillea robusta* (Silky Oak) Leaves by Soda-Anthraquinone Pulping Using Response Surface Methodology. *Green and Sustainable Chemistry*, **14**, 43-65.
https://doi.org/10.4236/gsc.2024.143004

Received: April 21, 2024
Accepted: July 1, 2024
Published: July 4, 2024

Abstract

Response surface methodology (RSM) using the central composite design (CCD) was applied to examine the impact of soda-anthraquinone pulping conditions on *Grevillea robusta* fall leaves. The pulping factors studied were: NaOH charge 5% to 20% w/v, pulping time 30 to 180 minutes, and the anthraquinone charge 0.1 to 0.5% w/w based on the oven-dried leaves. The responses evaluated were the pulp yield, cellulose content, and the degree of delignification. Various regression models were used to evaluate the effects of varying the pulping conditions. The optimum conditions attained were; NaOH charge of 14.63%, 0.1% anthraquinone, and a pulping period of 154 minutes, corresponding to 20.68% pulp yield, 80.56% cellulose content, and 70.34% lignin removal. Analysis of variance (ANOVA), was used to determine the most important variables that improve the extraction process of cellulose. The experiment outcomes matched those predicted by the model (Predicted R^2 = 0.9980, Adjusted R^2 = 0.9994), demonstrating the adequacy of the model used. FTIR analysis confirmed the elimination of the non-cellulosic fiber constituents. The lignin and hemicellulose-related bands (around 1514 cm^{-1}, 1604 cm^{-1}, 1239 cm^{-1}, and 1734 cm^{-1}) decreased with chemical treatment, indicating effective cellulose extraction by the soda-anthraquinone method. Similar results were obtained by XRD, SEM and thermogravimetric analysis of the extracted cellulose. Therefore, *Grevillea robusta* fall leaves are suitable renewable, cost-effective, and environmentally friendly non-wood biomass for cellulose extraction.

Keywords

Cellulose Extraction, Response Surface Methodology, Central Composite Design, Delignification

1. Introduction

The environmental concerns, scarcity of trees, and rising worldwide demand for fibrous materials have resulted in non-wood fibers being one of the most significant alternate resources available today [1] [2]. The non-wood fibers are obtained from renewable resources, including biomass from agricultural and forestry feedstock, which are generated after crop harvesting. Fall leaves are biodegradable and composted naturally in forests, however, they are trash in cities [3]. These biomasses are categorized as lignocelluloses, which consists of cellulose (38% - 50%), hemicellulose (17% - 32%), and lignin (15% - 30%) in their cell walls [4] [5]. In addition to these components, other low-molecular compounds, known as micromolecules are also present. Lignin is composed of polyphenol aromatics, while pentose and hexose sugar monomers combine to form cellulose and hemicellulose.

The most prevalent and important polysaccharide is cellulose, which is made up of hundreds of glucose molecules that are present in plant cell walls as microfibrils. Cellulose has a high turnover rate and is known to be degradable and compatible with nature [6]. Lignin is a lignocellulose material that is comparatively challenging to break down. Its inclusion in lignocellulose materials restricts its application in industry. Strong connections are formed between lignin and carbohydrates. It is challenging to separate cellulose and hemicellulose during the fiber preparation process as a result of these linkages, which prohibit solutions or enzymes from dissolving them. Lignin presence in lignocellulose materials prevents cellulose from being used to its full potential. Therefore, delignification is required to separate lignocellulose into lignin, cellulose, and hemicellulose and remove the non-cellulosic components. Purification of cellulose is necessary because of its use in numerous processes, including the production of cellulose-based threads, films, textile fibers, building materials, adsorbents, gelling agents, thickeners and stabilizers in processed foods, packaging and wrapping materials, etc. [7].

The amount of cellulose in plants varies, depending on species, origin, maturity, and method of extraction [5]. There are many different techniques for delignifying materials, which include: chemical, physicochemical, mechanical, and biological [8]. Alkaline pretreatment is the most widely used pretreatment method for non-wood biomass before it is transformed into different derivative products. Alkali, particularly, sodium hydroxide, works well as a cellulose swelling agent and serves as the major delignifier in alkaline pulping techniques [9]. An earlier study found that a low concentration of alkali was sufficient for the

isolation of cellulose from lignocellulose biomass. Hemicellulose and lignin are hydrolyzed and made water-soluble in an alkaline solution [2].

Anthraquinone (AQ) is an important catalyst that is frequently utilized in the alkaline pulping of wood due to its ability to sustain pulp production and enhance delignification, even when added in a small proportion [10]-[12]. During alkaline pulping, it functions as a redox catalyst and converts the carbohydrates' reducing aldehyde end groups into carboxylic acids through oxidation. This oxidation of the aldehyde to carboxylic acid groups inhibits the stepwise alkaline depolymerization reaction that occurs with the reducing sugar end groups, boosting yield [10].

In this study, the soda-anthraquinone pulping method was used to extract cellulose from *G. robusta* leaves. To maximize pulp production, cellulose content, and delignification, the ideal NaOH charge, anthraquinone charge, and pulping time were determined using the Central Composite Design (CCD) of Response Surface Methodology (RSM). This method of optimization involves determining the best value for each relevant component to produce the best possible results from an experiment. Each response's objective was specified in the experimental design [13].

Grevillea robusta is often referred to as river oak, southern silky oak, silver oak, silky oak, or grevillea in English [14]. It is a common and fast-growing tree that produces a significant amount of leaf biomass quickly [15]. It has an added advantage because it can grow on coffee and tea farms, providing the required shade and humus without interfering with other plants in the immediate environment [16]. There is increasing interest globally, for use of environmentally-friendly, renewable and sustainable feedstock to mitigate growing climate change concerns. Leaf litter was selected for two reasons: first, it is a widely distributed annually renewable natural resource that requires little work to gather since it is done in the fall with a rake, and second, it is not currently employed for anything beneficial other than mulch creation. *G. robusta* leaf litter is therefore a desirable and affordable source of cellulose used in this study. Whereas, delignification of the bark of *Grevillea robusta* from Ethiopia has been reported [17]. In this study *Grevillea* fall leaves were used to extract the cellulose taking into account sustainable development goals. The study therefore aimed at optimizing the process of cellulose extraction from *G. robusta* fall leaves for conversion to other important industrial and domestic products such as biocomposites.

2. Materials and Methods

2.1. Materials

Grevillea robusta fall leaves were randomly collected from the tree plantations at the Kenya Forest Research Institute (KEFRI) in Muguga, Kiambu County, Kenya.

The reagents and chemicals used in the study included sodium hydroxide (NaOH, 99.5%) and sodium hypochlorite (NaOCl, 10%) from Euro Chemicals Ltd, Kenya. Potassium bromide (KBr, 99%) from High Pure Laboratory Chemi-

cals Pvt. Ltd. Commercial cellulose powder from Balston Ltd., England. Di-sodium hydrogen phosphate (99%) from Merk chemicals, ethylenediaminetetraacetic acid (EDTA 99%), Sodium lauryl sulphate (85%), 2-ethoxy ethanol (99%), N-ethyl-N,N,N-trimethyl ammonium bromide (CTAB, 98%) and Sulphuric acid (98%) from Loba chemicals. All the reagents were of analytical grade.

2.2. Material Preparation

The *G. robusta* leaves were washed in clean water, dried in the sun, and then packaged. Low water content in biomass results in high fiber content [18]. The dried leaves were then ground into small pieces of 300 µm using a mill and a vibratory sieve shaker (Techno test Modena-Italy mill, code: SS 205/2). The leaves were then stored in air-tight bags and kept in the laboratory ready for analysis.

2.3. Proximate Analysis

The AOAC Official Method 978.10 was employed to ascertain the crude fiber percentage of the leaves. The percentage of ash was calculated using the 2001 ASTM standard E1755. Moisture content was determined using the Tappi method T412 om-16. Cellulose, hemicellulose, and lignin contents of the samples were determined as described by Van Soest and Robertson's method [18] [19]. This method uses chemical reagents to examine materials and determine the presence of neutral detergent fiber (NDF), acid detergent fiber (ADF), and acid detergent lignin (ADL). After the digestion of sample in a neutral detergent solution, NDF whose principal components are cellulose, hemicellulose, and lignin was obtained. Acid detergent was used to break down NDF, resulting in ADF, which primarily comprises cellulose and lignin. Sulphuric acid was used to eliminate the cellulose from ADF to obtain ADL [3]. The quantities of lignin, hemicellulose, and cellulose were calculated using the following formula:

$$\%\,\text{Hemicellulose} = \text{NDF} - \text{ADF} \tag{1}$$

$$\%\,\text{Cellulose} = \text{ADF} - \text{residue of } 72\%\ \text{H}_2\text{SO}_4 \text{ treatment residue} \tag{2}$$

$$\%\,\text{Lignin} = \text{ADL} \tag{3}$$

2.4. Extraction of Cellulose from *G. robusta* Leaves

Soda-anthraquinone method was used for the delignification of *G. robusta* leaves. About 20 g of the oven-dried leaves were reacted with 500 ml of cooking liquor of soda-anthraquinone mixture in varying concentrations and pulping time. In this study, optimization of the influential parameters was as follows: alkali (NaOH) charge, 5% to 20% w/v [20], time, 30 to 180 minutes [21], and anthraquinone charge, 0.1% to 0.5% w/w [22] of the oven-dried samples. The fixed factors were a pulping temperature of 100˚C ± 5˚C and a sample mass to pulping liquor ratio of 1: 25 to ensure complete immersion of the sample. A high solid-to-liquor ratio is ideal because it promotes increased delignification due to availability of NaOH until the substrate/solvent system is saturated [23]. Pulp

samples were bleached in a 10% solution of sodium hypochlorite (NaOCl) in the alkaline medium for 2 hours at room temperature with continuous stirring using an electric stirrer. The bleached pulp was then washed to near-neutral pH and then dried at 105˚C in the oven to constant mass. Equations (4) and (5), were used to determine the degree of delignification and the pulp yield respectively [3].

$$\%\,\text{Deliginification degree} = \frac{\text{Total lignin in raw sample} - \text{Residue lignin in pulp}}{\text{Total lignin in raw sample}} \times 100 \quad (4)$$

$$\%\,\text{Pulp yield} = \frac{\text{Oven dry weight}(\text{g})\,\text{pulp}}{\text{Oven dry weight of raw sample}} \times 100 \quad (5)$$

2.5. Experimental Design and Optimization

Following an extensive literature review [9] [12] [18], the appropriate experimental working conditions were selected. By applying the response surface technique (RSM), a central composite-based experimental design (CCD) was created using the Design-Expert version 13.0 software by Stat-Ease, Inc. To create an empirical relationship between process factors and desired responses or product attributes, the response surface approach incorporates statistical and mathematical analyses of the results of experiments. It offers a comprehensive framework for the fitting of the model, process optimization, and data analysis [23]. **Table 1** displays the independent factors along with respective CCD levels.

Table 1. The levels of independent factors in CCD.

Independent variables	Code	Levels				
		$-\alpha$ (−1.682)	Low (−1)	Center (0)	High (+1)	$+\alpha$ (+1.682)
NaOH charge %	*A*	1.22745	6	13	20	24.7725
Pulping time min	*B*	5.68347	50	115	180	224.317
Anthraquinone charge %	*C*	0.04409	0.16	0.33	0.5	0.615905

Equation (6) was used to determine the total number of experiments:

$$N = 2^a + 2a + kc \quad (6)$$

The symbols *N*, *a*, and *Kc* represent the total number of experiments, variables and replicates, respectively [23].

Twenty experimental runs, including six replications at the center point, were carried out using the chosen pulping parameters range. The replicates at the center point give a pure error. The experimental sequencing was followed in the pulping order, enabling an entirely random pulping procedure. The experiments were performed in triplicates.

2.6. Model Fitting and Statistical Analysis

The experimental data were produced using design-expert software, and the regression model was created from the results. The regression coefficient value (R^2) represented the regression model's quality of fit. Pulp yield, cellulose content, and lignin removal were evaluated responses that were fitted to the second-order polynomial model. The effectiveness of the proposed model was evaluated using analysis of variance (ANOVA), with a 95% confidence level, taking into account the significance of each factor and its interactions [23].

Three-dimensional surface plots were used to describe each factor's impact as well as how the factors and responses interacted. The computational validation of the model was according to the examination of the estimated mistakes and the coefficients of determination (R^2) between the expected outcomes of the model and the experimental data. The maximum target for the three responses was reached using an optimization technique based on the desirability function [24]. After that, experimental data with a 95% confidence interval (CI) verified the RSM's optimal conditions prediction.

2.7. Characterization of Cellulose

2.7.1. The FTIR Analysis

The FTIR (Tensor 27 Bruker and Perkin Elmer) spectrophotometer was used to record the infrared spectra for characterization of the functional groups and chemical composition of the samples. The sample pellets were prepared by grinding the samples with KBr in the ratio of 1:100. The spectrum was scanned in transmittance mode at 32 scans per minute with a resolution of 4 cm^{-1} in the range of 400 to 4000 cm^{-1} wave number. The typical functional groupings and matching bands for each component in cellulose, hemicellulose, and lignin were compared to literature [24].

2.7.2. Morphological Analysis of the Cellulose

A scanning electron microscope (SEM) Tescan Vega 3 LMH, operated at 20 kV accelerating voltage, using a secondary electron detector (SED) and energy dispersive spectroscopy (EDS) was used. The samples were first carbon-coated with the Agar Turbo Carbon coater, thereby improving their conductivity before measurement. The impact of the various chemical treatments was evaluated by comparing the bleached fibers with the untreated ground leaves.

2.7.3. The X-Ray Diffraction (XRD) Analysis

A powder X-ray diffraction (PXRD) instrument was used. The XRD patterns were obtained at room temperature using a PANalytical X'Pert Pro powder diffractometer, coupled to a Pixel detector. The X-ray radiation source was Cu-Kα radiation (0.154 nm) operating at 40 kV and 40 mA conditions.

X-ray diffraction (XRD) analysis was carried out to gather XRD patterns at ambient temperature and to learn more about the crystal structure. One of the most significant quantifiable characteristics of cellulose that determines its en-

zymatic digestibility is crystallinity, which is a measure of the weight percentage of the crystalline regions. The crystallinity index of the samples was calculated using the following formula:

$$\%\,\text{Crystallinity index} = \frac{\text{Area of crystalline peaks}}{\text{Area of the total domain}\left(\text{crystalline and amorphous peaks}\right)} \times 100 \quad (7)$$

2.7.4. Thermogravimetric Analysis

The thermostability of the untreated and the treated fibers was studied using a thermogravimetric analyser (TGA Q500 1732). The sample amount used was about 10mg. All measurements were performed under a nitrogen atmosphere with a gas flow of 100 ml/min and heated from 50˚C to 900˚C at a rate of 10˚C/min.

3. Results and Discussion

3.1. Proximate Study of *Grevillea robusta* Leaves Fiber

The main chemical components of *G. robusta* fall leaves are cellulose 37.6%, hemicellulose 12.23%, lignin 28.9%, crude fiber 48.68%, moisture content 9.46% and ash 6.44%. Table 2 illustrates that the cellulose content in *G. robusta* fall leaves is comparable to some other leaf biomass.

Table 2. Comparison of the chemical composition of untreated *G. robusta* fall leaf fibers with that of other plant leaf fibers.

Lignocellulose biomass	Cellulose %	Hemicellulose %	Lignin %	Reference
Wasted fall leaves	30.10	29.50	26.90	[3]
Pandanus tectorius leaves	37.30	34.40	22.60	[25]
Pandanus amaryllifolium leaves	48.79	19.95	18.64	[26]
Ficus (peepal tree) leaves	38.10	23.40	4.50	[27]
Cymbopogan citratus leaves	37.56	29.29	11.14	[28]
Grevillea robusta leaves	37.60	12.23	28.90	Present work

Lignocellulosic material is considered a potential raw material for pulping when they have higher than 34% cellulose content [9]. Therefore, *G. robusta* fall leaves with 37.6% cellulose content are a promising basic substance for pulp extraction.

When soda-AQ pulping was carried out on oven-dried *G. robusta* leaves, an average pulp yield of about 20.86 ± 1.43% was obtained. This amount of yield is close to 26.25 ± 1.6% obtained from *Calathealutea* leaves by Bolio *et al*, [27]. The lowest yield was obtained when the main pulping parameters, usually, time and NaOH charge were at the maximum value (19.24%). High alkali charge and prolonged time cause more degradation of pulp leading to low yield [12]. The fall leaves, raw sample, unbleached, and bleached cellulose are shown in Figure 1.

Figure 1. Images of (a) fall leaves, (b) raw sample, (c) unbleached cellulose, and (d) bleached cellulose.

3.2. Optimization

The ideal conditions for cellulose extraction were determined by evaluation of the effects of the process variables (NaOH charge, anthraquinone charge, and pulping time) and their correlation with the expected responses using Response Surface Methodology (RSM). **Table 3** displays the full design matrix along with the obtained responses.

Table 3. Central composite design for NaOH-AQ pulping and the experimental responses.

STD	Run	Level of factors [Actual (coded)]			Responses		
		Factor 1	Factor 2	Factor 3	Response 1	Response 2	Response 3
Std	Run	A: NaoH charge	B: Pulping time	C: Anthraquinone charge	Pulp yield	Cellulose content	Lignin removal
		%	min	%	%	%	%
19	1	13 (0)	115 (0)	0.33 (0)	23.68	77.76	68.6
9	2	1.23 (−1.68)	115 (0)	0.33 (0)	24.85	65.41	56.89
7	3	6 (−1)	180 (1)	0.5 (1)	23.79	76.76	66.88

Continued

18	4	13 (0)	115 (0)	0.33 (0)	23.66	77.83	68.52
3	5	6 (−1)	180 (1)	0.16 (−1)	21.6	73.78	65.57
13	6	13 (0)	115 (0)	0.04 (−1.68)	21.83	75.56	66.13
8	7	20 (1)	180 (1)	0.5 (1)	21.05	91.64	67.73
10	8	24.8 (1.68)	115 (0)	0.33 (0)	20.97	89.47	70.48
4	9	20 (1)	180 (1)	0.16 (−1)	19.24	87.7	71.81
11	10	13 (0)	5.7 (−1.68)	0.33 (0)	24.69	67.51	60.83
17	11	13 (0)	115 (0)	0.33 (0)	23.71	77.85	68.52
16	12	13 (0)	115 (0)	0.33 (0)	23.71	77.84	68.59
20	13	13 (0)	115 (0)	0.33 (0)	23.64	77.85	68.52
5	14	6 (−1)	50 (−1)	0.5 (1)	25.31	65.97	60.27
2	15	20 (1)	50 (−1)	0.16 (−1)	22.88	77.61	67.78
6	16	20 (1)	50 (−1)	0.5 (1)	23.14	80.51	70.11
14	17	13 (0)	115 (0)	0.6 (1.68)	24.03	80.48	69.05
12	18	13 (0)	224.3 (1.68)	0.33 (0)	20.34	85.11	69.82
1	19	6 (−1)	50 (−1)	0.16 (−1)	24.57	63.87	52.54
15	20	13 (0)	115 (0)	0.33 (0)	23.65	77.78	68.56

The pulp yield data in Table 3 was fitted to two-factor interaction (2FI), cubic, quadratic, and linear polynomials. Table 4 displays the results.

Table 4. Summary statistics of the model for pulp yield.

Source	Sequential p-value	Lack of Fit p-value	Adjusted R^2	Predicted R^2	
Linear	<0.0001	<0.0001	0.8747	0.8420	
2FI	0.2515	<0.0001	0.8862	0.7965	
Quadratic	<0.0001	0.1518	0.9994	0.9980	Suggested
Cubic	0.2921	0.1039	0.9995	0.9844	Aliased

The quadratic model was selected, as seen in Table 4, to be the most appropriate for predicting the optimum conditions for cellulose extraction. The predicted R^2 for the model (0.9991) is compliant with the adjusted R^2 (0.9994) with a deviation of less than 0.2, indicating that the model is adequate.

3.3. Analysis of variance

ANOVA was used in the experiment design to gauge the model's accuracy based on the experimental findings [29]. Table 5 presents the ANOVA results, which show that the pulp yield is considerably impacted by the process factors under investigation.

Table 5. ANOVA for the pulp yield quadratic model.

Source	Sum of Squares	df	Mean Square	F-value	p-value	
Model	51.02	9	5.67	2904.07	< 0.0001	significant
A-NaOH charge	17.56	1	17.56	8995.07	< 0.0001	
B-Pulping time	22.52	1	22.52	11534.88	< 0.0001	
C-Anthraquinone charge	5.54	1	5.54	2839.19	< 0.0001	
AB	0.1922	1	0.1922	98.46	< 0.0001	
AC	0.0925	1	0.0925	47.36	< 0.0001	
BC	1.12	1	1.12	576.32	< 0.0001	
A^2	1.12	1	1.12	575.68	< 0.0001	
B^2	2.53	1	2.53	1295.48	< 0.0001	
C^2	1.07	1	1.07	546.90	< 0.0001	
Residual	0.0195	10	0.0020			
Lack of Fit	0.0121	5	0.0024	1.64	0.3007	not significant
Pure Error	0.0074	5	0.0015			
Cor Total	51.04	19				

Based on its F-value of 2904.07, as shown in Table 5, the model is deemed relevant. Compared to the pure error, the 1.64 Lack of Fit F-value suggests that the Lack of Fit is not statistically significant. A considerable regression and an insignificant lack of fit are characteristics of an acceptable model. Significant model terms are indicated by P-values less than 0.0500. Relevant model terms in this study are *A*, *B*, *C*, *AB*, *AC*, *BC*, A^2, B^2, and C^2.

The second-order polynomial equations correlating pulp yield, cellulose content, and lignin removal to the independent process variables were developed (eq. 8, 9, and 10). From the model equations, all three independent variables (NaOH charge, anthraquinone charge, and time) had a significant influence on all the responses. The final equations concerning the coded factors are,

$$\%\,\text{Pulp yield} = 23.68 - 1.13A - 1.2B + 0.637C - 0.155AB - 0.1075AC + 0.375BC - 0.279A^2 - 0.4189B^2 - 0.2722C^2 \quad (8)$$

$$\%\,\text{Cellulose} = 77.82 + 7.14A + 5.24B + 1.48C + 0.065AB + 0.22AC + 0.24BC - 0.132A^2 + 0.532B^2 + 0.0729C^2 \quad (9)$$

$$\%\,\text{Delignification} = 68.55 + 4.03A + 2.67B + 0.893C - 2.25AB - 1.35AC - 1.6B\ \ 1.72A^2 - 1.14B^2 - 0.343C^2 \quad (10)$$

3.4. Model Accuracy

It is crucial to check the model adequacy in order to ascertain its validity. The plots of residuals for the responses lie approximately on a straight line and shows no deviation of the variance (Figure 2). The plots of predicted versus ac-

tual (simulated) show a strong linearity as shown in Figure 3. The results for the two plots indicate that the responses could be adequately described by the established model [30].

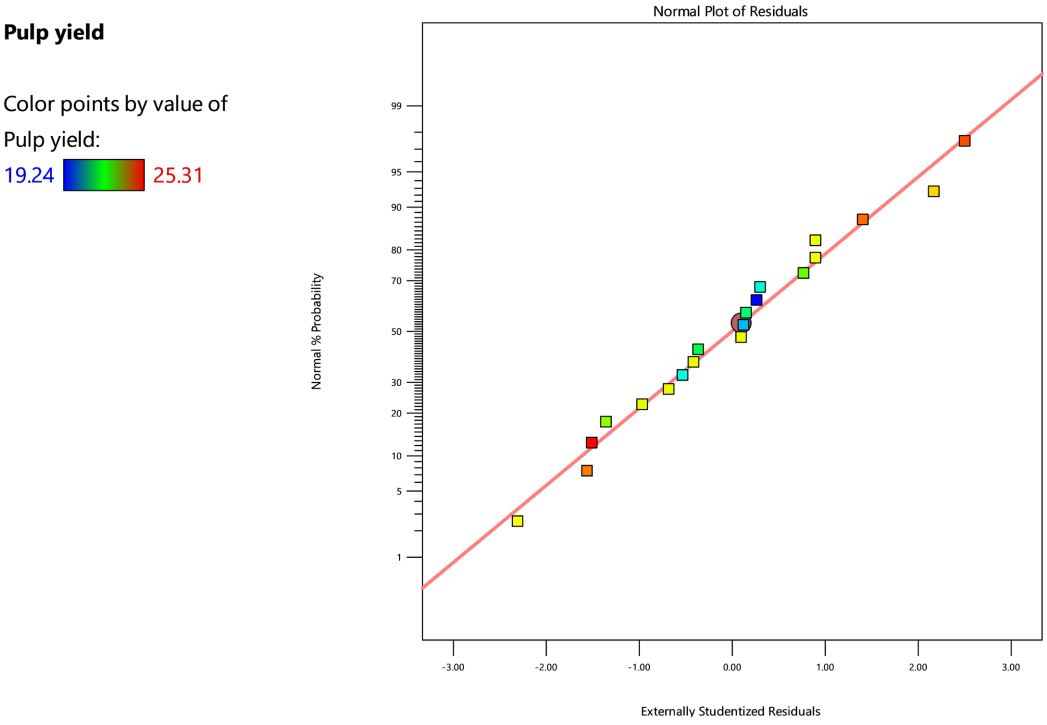

(2a) For % yield

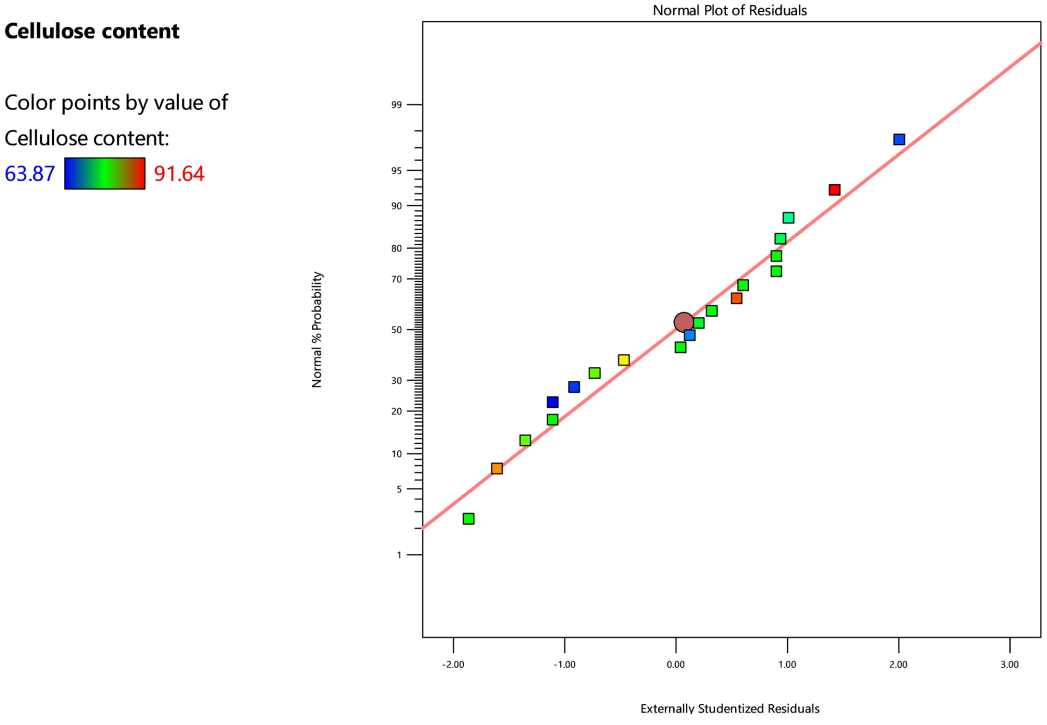

(2b) For % cellulose

Figure 2. The plots of externally studentized residuals (2a), for yield and (2b), for cellulose content.

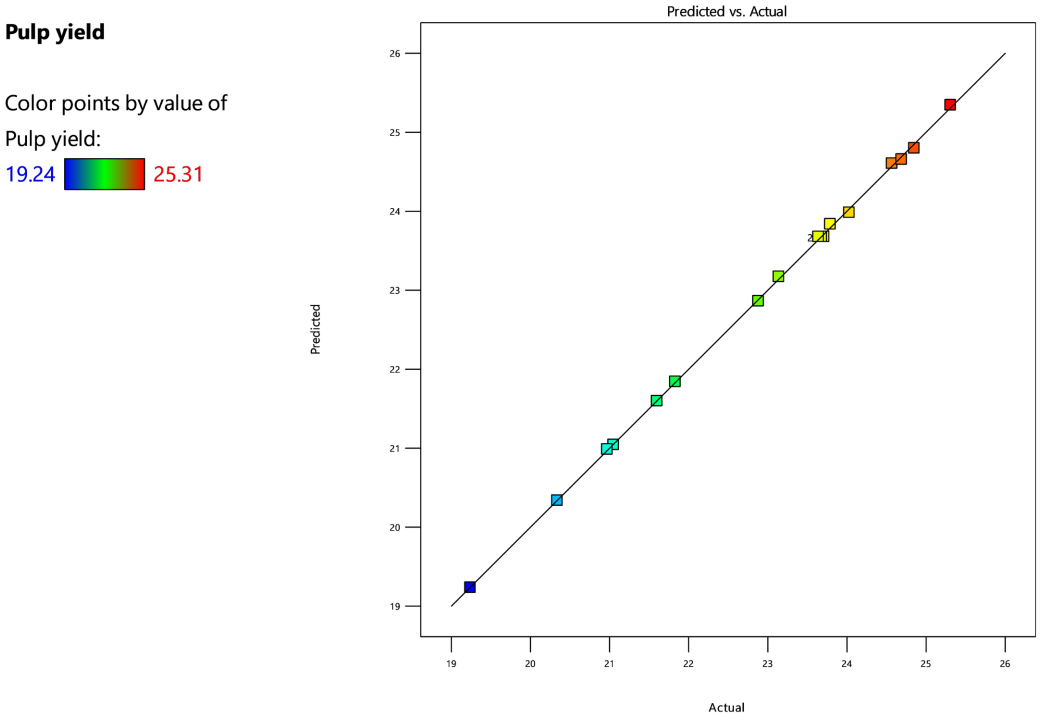

(3a) For % yield

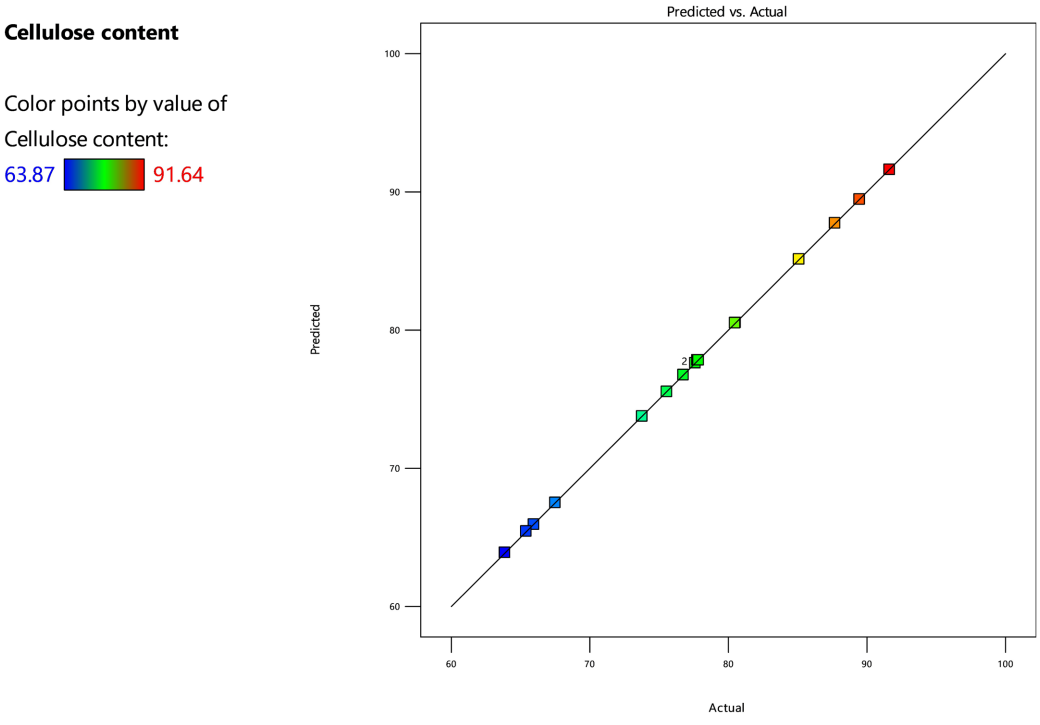

(3b) For % cellulose

Figure 3. Graph of predicted against actual (simulated) data for (3a), pulp yield and (3b), cellulose content.

3.5. Response surface plots

Further, the response surface methodology was applied to plot both two- and three-dimensional plots for graphical representation of the model formulations

derived from the data evaluation. This is significant when evaluating the impact of multiple factors, particularly those with intricate interconnections [23]. **Figures 4-6** show 3-D graphical representation of the model of responses (pulp yield, cellulose content, and lignin removal) against the NaOH and anthraquinone charge.

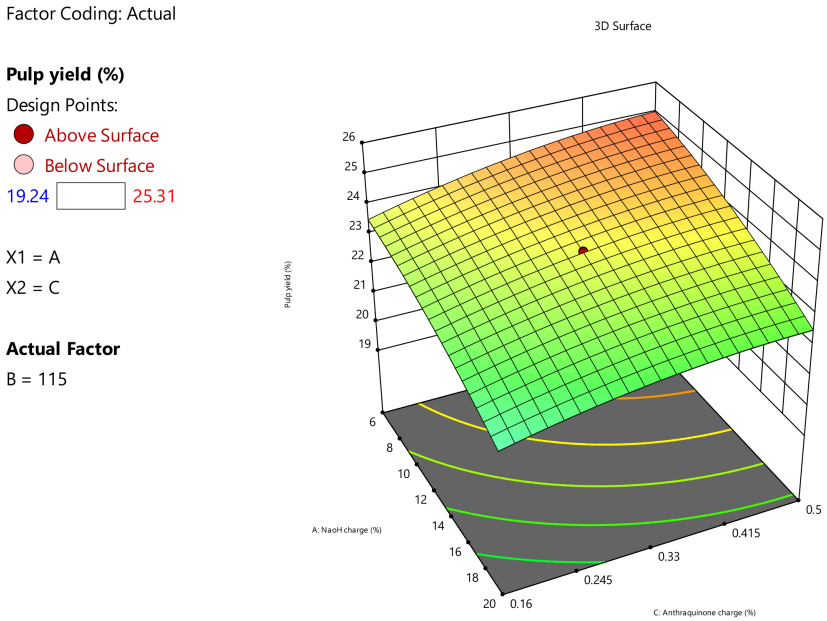

Figure 4. 3D-response surface plot for the model of % pulp yield against NaOH charge and anthraquinone charge.

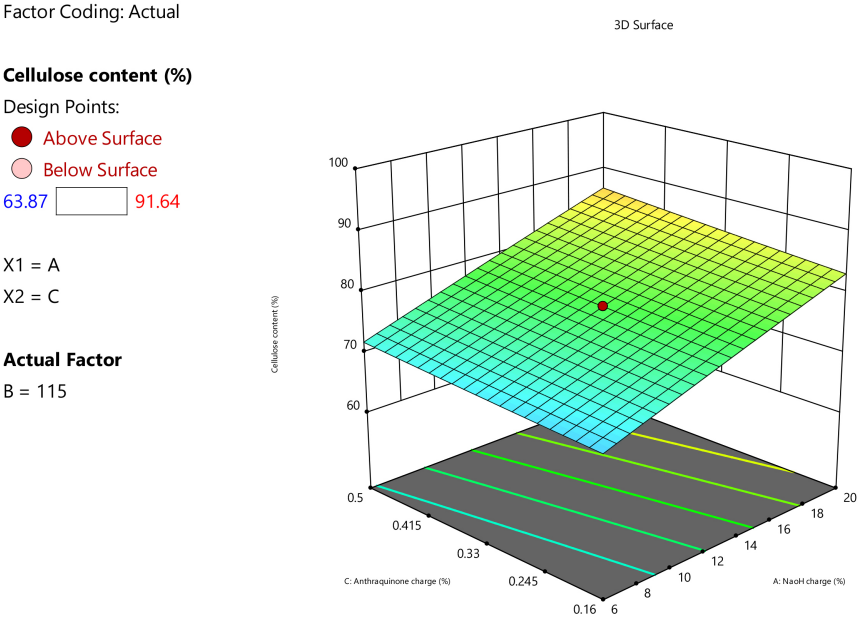

Figure 5. 3D-response surface plot for the model of % cellulose content against NaOH charge and anthraquinone charge.

The pulp yield shows a quadratic dependence on the NaOH charge. An in-

crease in NaOH charge therefore resulted in more dissolution of the non-cellulosic contents (lignin and hemicellulose) hence a decrease in pulp yield. Higher availability of anthraquinone resulted in enhanced lignin removal and lower degradation of cellulose. The yield therefore increased gradually with additional anthraquinone in the pulping liquor.

The cellulose content indicated a weak quadratic dependence on the NaOH charge and AQ charge. The %cellulose increased with an increase in NaOH and the anthraquinone charge respectively. However, there was a diminishing %increase with an increase in pulping time as more non-cellulosic contents continued to dissolve in the liquor which was observed as a black solution.

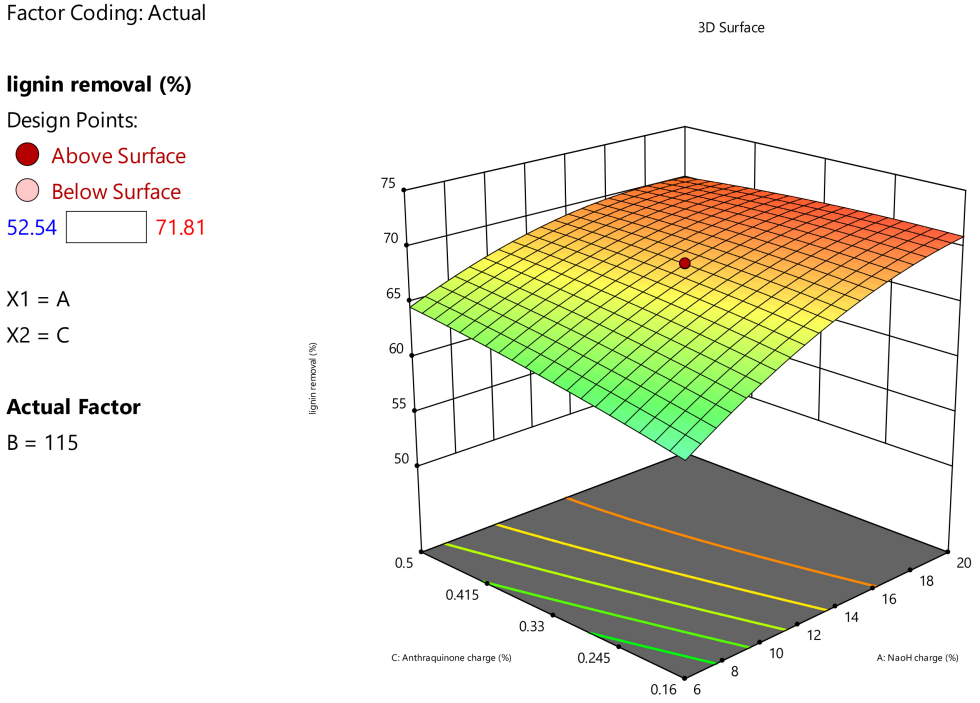

Figure 6. 3D-response surface plot for the model of % lignin removal against NaOH charge and anthraquinone charge.

Lignin removal displayed a strong quadratic relationship with the NaOH and anthraquinone charge in the pulping liquor. An increase in NaOH and anthraquinone charge resulted in more lignin dissolution. As more and more NaOH and anthraquinone were added, the extent of delignification reduced with time as more of the lignin was already dissolved.

In retrospect, **Figure 3**, **Figure 5**, and **Figure 6** show that when NaOH charge increases, pulp output reduces and lignin removal increases significantly, which leads to a rise in cellulose content. This is because alkaline hydrolysis decreases the quantity of non-cellulosic materials by breaking the bonds between aryl-ether, carbon-carbon, and aryl-aryl functional groups and the ester groups between lignin and hemicellulose [13].

The desirability methodology was used to optimize the responses. This approach converts the response to a specific desirability function. The desirability

function ranges from 0 to 1, where 0 represents an undesired outcome and 1 represents the optimal preferred outcome [23]. The constraints of the factors were kept on range and the preferred charge of anthraquinone was set at 0.1 as a recommendation by the Food and Drug Administration (FDA) in the US on anthraquinone usage in lignocellulosic pulping [12]. The optimum conditions for cellulose extraction from *G. robusta* leaves achieved were 14.63% NaOH charge, 0.1% anthraquinone charge, and a pulping time of 154 minutes. The corresponding predicted values for the responses were; pulp yield of 20.68%, cellulose content of 80.56%, and lignin removal of 70.34%. These conditions were attained with a desirability of 1.

Subsequently, the experiment was run in triplicate with the process parameters set at optimum (14.63% NaOH, 0.1% AQ charge, and 154 minutes) to confirm the accuracy of the RSM model's output [29]. The obtained results were an average pulp yield of 20.86 ± 1.43%, cellulose content of 80.47%, and lignin removal of 70.59%. This was consistent with the expected outcomes. The findings imply that the model can, therefore, be used to optimize the variables used in the procedure for extraction of cellulose from *G. robusta* leaves.

3.6. FTIR analysis

The FTIR spectra for the *G. robusta* raw leaves, unbleached pulp, bleached pulp, and cellulose standard are displayed in **Figure 5**. Every spectra showed peaks at around 3336 cm^{-1} and 2917 cm^{-1} which are attributed to O-H and C-H bonds stretching vibrations of polysaccharides respectively [31].

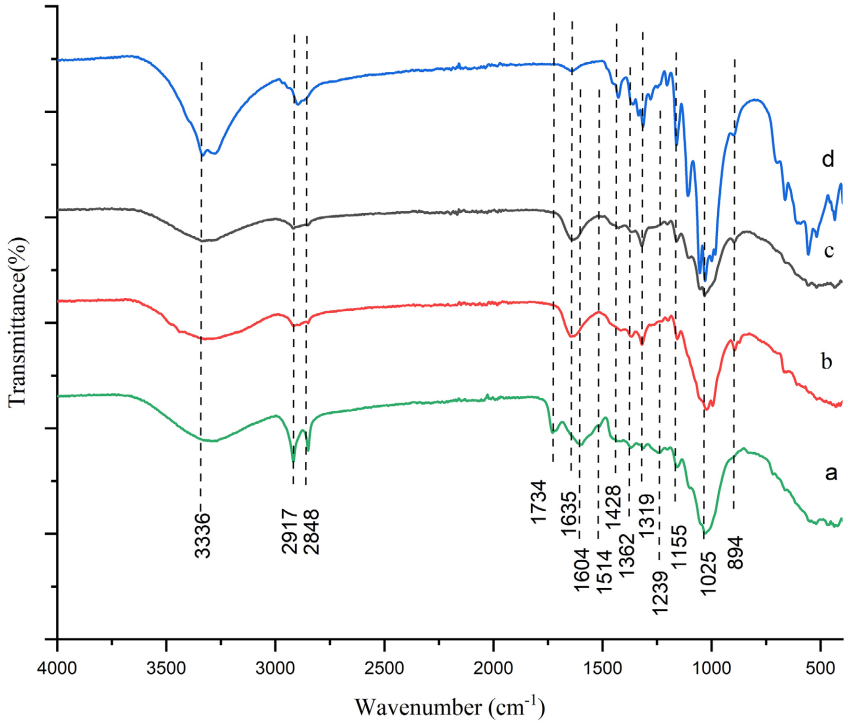

Figure 7. FTIR spectra for (a) untreated sample, (b) unbleached pulp, (c) bleached pulp, and (d) cellulose standard.

The band around 1428 cm^{-1} is due to CH_2 bending vibration, and around 1362 cm^{-1} are attributed to the C-H bending of cellulose. The absorption band at around 1319 cm^{-1} corresponds to C-C and C-O skeletal vibrations of cellulose [27]. The band around 1025 cm^{-1} is due to the stretching vibration of C-O and O-H bonds in the pyranose ring [26]. The band around 1155 cm^{-1} corresponds to C-O-C asymmetrical stretching [31]. The band around 894 cm^{-1} corresponds to β-glycosidic bonds between sugar units in cellulose [13] [32]. The band around 1635 cm^{-1} corresponds to O-H bending due to absorbed water [32]. The bands at around 1428 cm^{-1} and 894 cm^{-1} provide information about the amount of crystalline and amorphous regions of cellulose respectively The peaks approximately at 1734 cm^{-1} and 1239 cm^{-1} correspond to C=O stretching vibration due to the presence of the carbonyl aldehyde group and the -COO vibration of the acetyl group respectively, in hemicellulose of the leaf fibers [31]. The peaks decreased significantly after chemical treatment confirming the effective removal of hemicellulose. The bands around 1514 cm^{-1} and 1604 cm^{-1} correspond to aromatic skeletal vibrations in lignin [31]. The efficient removal of lignin and hemicellulose from leaf biomass is confirmed by the reduction of these peaks in the fibers treated with chemicals [33].

3.7. Scanning Electron Microscopy Study

The results in **Figures 8(a)-(c)** are micrographs taken to examine the effect of various treatments on surface morphology of the extracted cellulose.

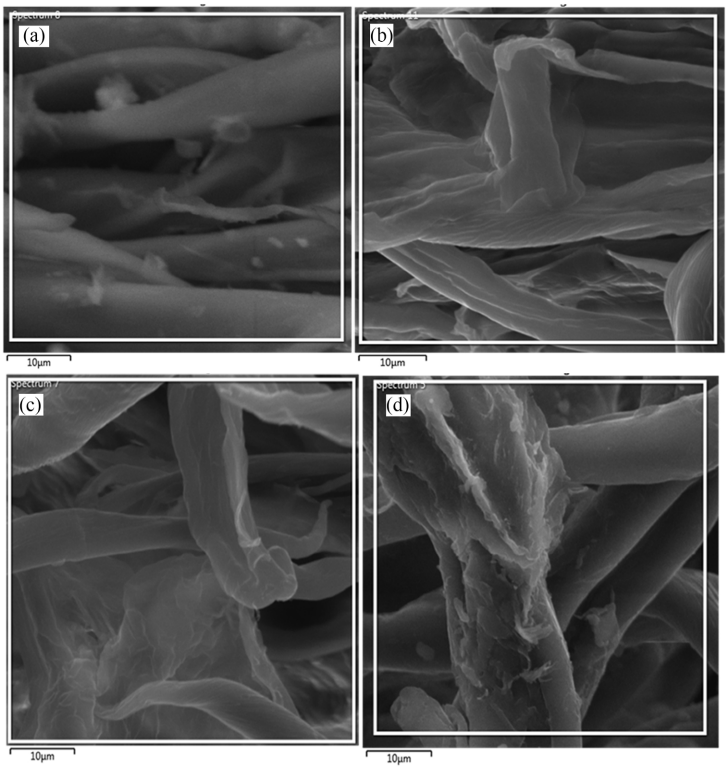

Figure 8. SEM Micrograph for (a) untreated sample, (b) unbleached cellulose, (c) bleached cellulose, and (d) cellulose standard.

The SEM results of **Figure 8(a)**, indicates that the surface of the cellulose fibers of the raw leaves is relatively smooth and intact. This is due to the binding of the fibers with, hemicellulose and lignin and the covering with wax and pectin on the surface. After treatment with NaOH and anthraquinone, hemicellulose and lignin are removed resulting in rough surface of cellulose fibers as observed in **Figure 8(b)**. After bleaching with NaOCl (**Figure 8(c)**), the fibers surface became rougher due to continued removal of wax, pectin, hemicellulose and lignin [13] [26]. This is evident with the increased surface area of the fibers. Further treatment resulted in cleavage of the fibers into smaller sizes [34]. The structures for the unbleached and bleached cellulose are comparable to that of cellulose standard (**Figure 8(d)**). The rough fiber surface shows a good ability to bind with other components for composite formation [35]. The micrographs displayed that most of the lignin and hemicellulose and surface impurities were removed by hydrolysis and depolymerisation and the fibrils were then produced by defibrillation of the original fibers.

3.8. XRD Analysis of Cellulose

The XRD results showed three distinct diffraction peaks at about $2\theta = 16.53^{\circ}$, 22.84˚, and 34.75˚, for the samples, which corresponds to the crystallographic planes of (110), (200) and (040), indicating the cellulose-1 structure. This revealed that the samples had a crystalline structure denoted as cellulose-1 [35].

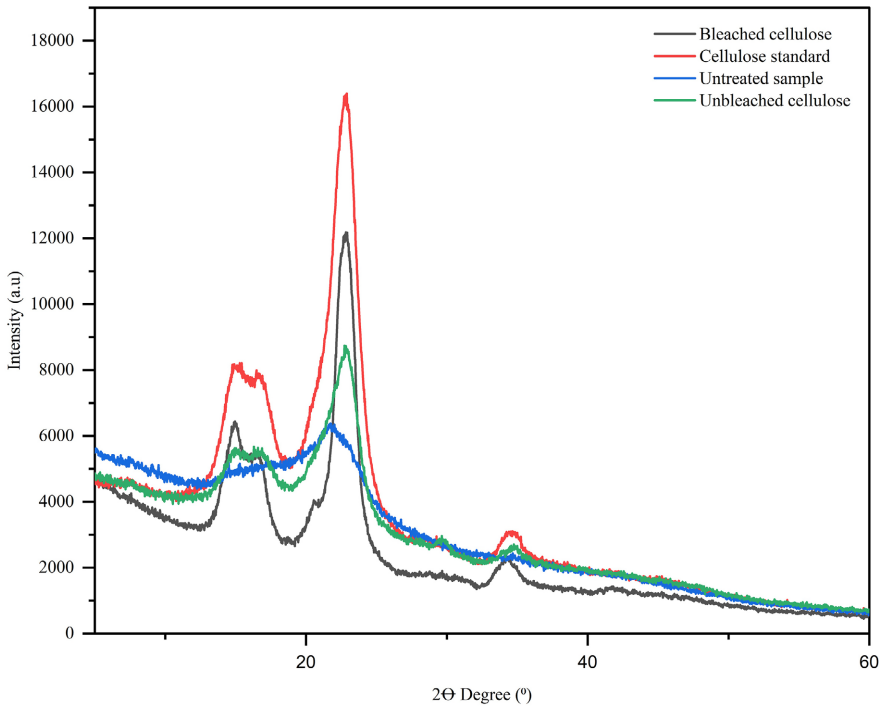

Figure 9. Comparison of XRD spectra of 300 μm Untreated sample, unbleached and bleached pulp

High crystallinity value is identified by the sharpness of the diffraction peaks,

where the sharper peak indicates high degree of crystallinity which might be due to cellulose rigidity [26]. As the amount of chemical treatment increased, the peak at 22.84˚ became sharper and narrower as demonstrated by the bleached pulp diffractogram in **Figure 9**. This demonstrated the removal of the amorphous content mainly, lignin and hemicellulose, raising the level of crystallinity and tensile strength of the fibers [13]. The untreated sample comprises amorphous and crystalline regions. The hemicellulose corresponds to the amorphous part, while lignin conjugated to cellulose includes both the amorphous and crystalline regions in biopolymers.

The elimination of lignin and hemicellulose components resulted in increased crystallinity index for the extracted cellulose. The calculated crystallinity index for the untreated sample, unbleached and bleached cellulose, and the standard cellulose are 42.34, 59.56, 74.66, and 82.43 respectively using the XRD amorphous subtraction method (as shown in **Table 6**) [36].

Table 6. Crystallinity index of the raw sample, unbleached sample, bleached sample and cellulose standard.

Sample	2Θ Amorphous (˚)	2Θ Crystalline (˚)	Crystallinity Index (%)
Raw sample	16.90	22.12	42.34
Unbleached cellulose	16.53	22.94	59.56
Bleached cellulose	16.53	22.89	74.66
Cellulose standard	16.84	22.9	82.43

The observed high crystallinity index implies crystalline nature, which is suitable for use of the fibers as an efficient reinforcement in composites [36].

3.9. Thermogravimetric Analysis

Figure 10 shows the thermograms of cellulose standard, untreated sample, unbleached and bleached cellulose. The thermal analysis is used to measure the weight degradation as the material is heated. Theoretically, cellulose degradation occurs due to dehydration and depolymerisation. The degradation temperature of lignin, hemicellulose and cellulose are within the temperature ranges of 160 - 900˚C, 220 - 315˚C and 315 - 400˚C respectively [35]. **Figure 8** displays three degradation phases of the cellulosic fibers: The first is the evaporation of volatile chemicals and absorbed water [35]. This phase is indicated by a minor weight loss around 100˚C due to the absorbed moisture loss by evaporation associated with the hydrophilic nature of lignocellulosic materials. The weight loss around this temperature was about 5% for all the samples. The second, is the hemicellulose and amorphous cellulose decomposition characterized by a major weight loss in the range of 250 - 385˚C. The most degradation occurred in this stage due to decomposition of cellulose. This thermal degradation corresponds to the cleavage of glycoside bonds in cellulose structure and depolymerisation of lignin. The final stage involves the crystalline cellulose and lignin decomposition from

420˚C to about 610˚C [33]. The final stage follows until the maximum temperature is achieved.

The % char residue at 650˚C was 21.8% for unbleached cellulose, 14.14% for bleached cellulose and 6.463% for cellulose standard. The percentage char residue in bleached cellulose is lower than the unbleached cellulose. This is due to removal of ash which is in agreement with chemical analysis [27].

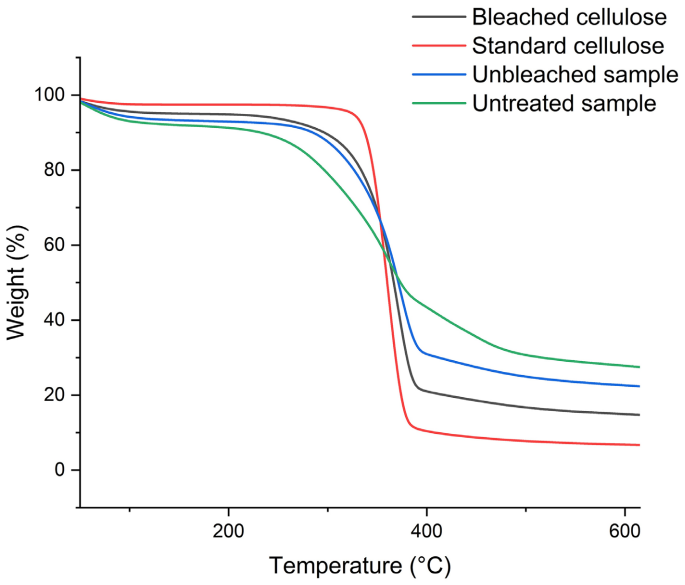

Figure 10. Primary thermograms for untreated sample, unbleached, bleached and standard cellulose.

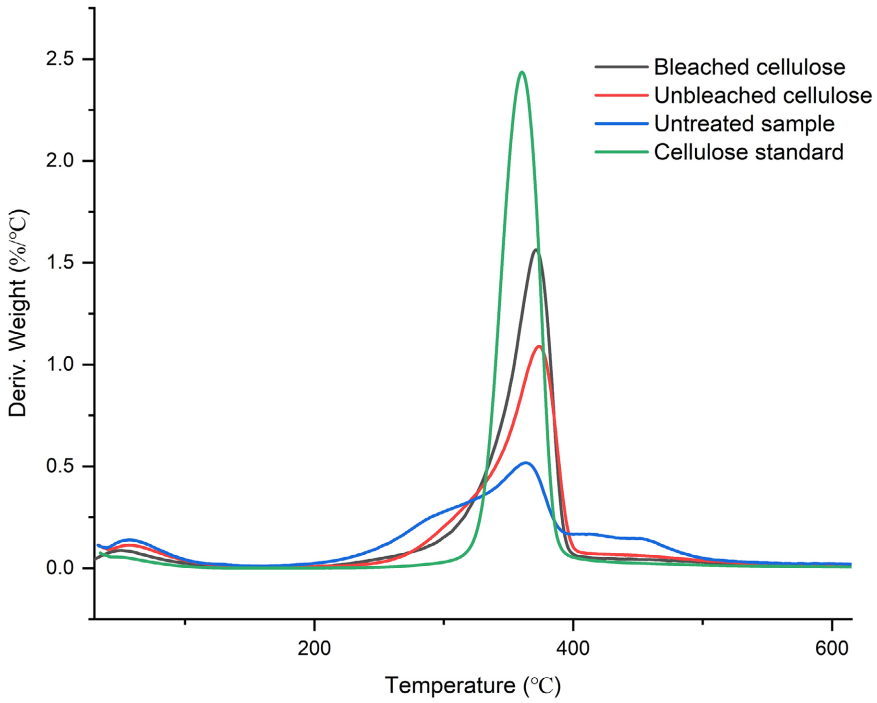

Figure 11. DTG thermograms for untreated sample, unbleached, bleached and standard cellulose.

The DTG thermograms in Figure 11, displayed the first peaks at around 100˚C, corresponding to the loss of moisture. The second prominent peak occurred in the temperature range between 210˚C and 380˚C. This peak corresponds to the degradation of cellulose [35]. The untreated sample displayed exceptional decomposition peaks at 220 - 298˚C and at 410 - 500˚C which is due to decomposition of hemicellulose and lignin respectively [35]. These peaks are missing in the extracted cellulose, due to the removal of the amorphous content during chemical extraction.

Table 7. Thermal degradation temperatures of the untreated sample, unbleached cellulose, bleached cellulose, and cellulose standard.

Samples	T_{Onset} (˚C)	T_{Max} (˚C)	Residue at 650˚C (%)
Raw sample	266.6	364.4	26.68
Unbleached sample	283.9	376.7	21.98
Bleached sample	301.4	373.2	14.14
Cellulose standard	331.2	361.6	6.463

According to Table 7, the obtained thermostability temperature in Figure 10, is 266.6˚C for the untreated sample, 283.9˚C for the unbleached cellulose, and 301.4˚C for the bleached cellulose. This is close to the standard cellulose which gave a thermal degradation temperature of 331.2˚C. The chemical treatment resulted in an increase in the stability of the fiber because of the retention of the structural order and removal of the amorphous content [33].

4. Conclusion

The study resulted in the development of a method for extracting cellulose from *Grevillea robusta* leaves. The major variables for extraction of cellulose fibers were determined (14.63% NaOH charge, 0.1% anthraquinone charge, and pulping time of 154 minutes), the optimum pulp yield was 20.68% with 80.56% cellulose content and 70.34% lignin removal. Characterization of the obtained cellulose was carried out by FTIR analysis of the functional groups using the cellulose standard as the reference. The decrease and disappearance of the peaks associated with lignin and hemicellulose confirmed the effectiveness of the extraction process. The bleached cellulose had higher crystallinity than the unbleached and untreated leaf samples. The thermogravimetric analysis gave the thermal stability of the extracted cellulose up to 301.4˚C, which is high and within the polymerization process temperature conditions. The obtained results in this study confirmed that the *G. robusta* fall leaves, which are agricultural waste, are suitable renewable, cheap, and environmentally friendly biomass for cellulose extraction. Furthermore, the extracted cellulose can be utilized to make biocomposite polymers which can go a long way in alleviating environmental pollution due to the use of fossil-based polymers.

Acknowledgements

The authors would like to express their gratitude to the National Research Fund (NRF) for funding this study under grant number NRF/1/PhD/517.

Conflicts of Interest

The authors declare no conflicts of interest regarding the publication of this paper.

References

[1] Paridah, M.T., Juliana, A.H., Zaidon, A. and Abdul Khalil, H.P.S. (2015) Nonwood-Based Composites. *Current Forestry Reports*, **1**, 221-238. https://doi.org/10.1007/s40725-015-0023-7

[2] Hapani, U., Highland, H.N., Solanki, H. and George, L. (2021) Extraction of Cellulose from Lignocellulosic Biomass. *Ecology Environment and Conservation*, **27**, S358-S364. https://www.researchgate.net/publication/350196339

[3] Atici, O.G. and Tezcan, E. (2017) Isolation of Cellulose and Hemicellulose by Using Alkaline Peroxide Treatment at Room Temperature from Wasted Fall Leaves. *Polymer International*, **2**, 100-110.

[4] Sankaran, R., *et al*. (2021) The Expansion of Lignocellulose Biomass Conversion into Bioenergy via Nanobiotechnology. *Frontiers in Nanotechnology*, **3**, 1-10. https://doi.org/10.3389/fnano.2021.793528

[5] Husin, M., Rahim, N., Ahmad, M.R., Romli, A.Z. and Ilham, Z. (2019) Hydrolysis of Microcrystalline Cellulose Isolated from Waste Seeds of Leucaena Leucocephala for Glucose Production. *Malaysian Journal of Fundamental and Applied Sciences*, **15**, 200-205. https://doi.org/10.11113/mjfas.v15n2.1165

[6] Melesse, G.T., Hone, F.G. and Mekonnen, M.A. (2022) Extraction of Cellulose from Sugarcane Bagasse Optimization and Characterization. *Advances in Materials Science and Engineering*, **2022**, Article ID: 1712207. https://doi.org/10.1155/2022/1712207

[7] Hapani, U., Highland, H. and George, L.B. (2020) Eco-Friendly Extraction and Characterization of Cellulose from Fenugreek (*Trigonella foenum-gracum* L.) Stem. *Journal of Experimental Biology and Agricultural Sciences*, **8**, 479-488. https://doi.org/10.18006/2020.8(4).479.488

[8] Tocco, D., Carucci, C., Monduzzi, M., Salis, A. and Sanjust, E. (2021) Recent Developments in the Delignification and Exploitation of Grass Lignocellulosic Biomass. *ACS Sustainable Chemistry & Engineering*, **9**, 2412-2432. https://doi.org/10.1021/acssuschemeng.0c07266

[9] Zendrato, H.M., Devi, Y.S., Masruchin, N. and Wistara, N.J. (2021) Soda Pulping of Torch Ginger Stem: Promising Source of Nonwood-Based Cellulose. *The Journal of the Korean Wood Science and Technology*, **49**, 287-298. https://doi.org/10.5658/WOOD.2021.49.4.287

[10] Fišerová, M., Gigac, J. and Melník, P. (2006) Application of Anthraquinone in Kraft Pulping of Beech Wood. *Wood Research*, **51**, 55-68.

[11] Ferrer, A., Vargas, F., Jameel, H. and Rojas, O.J. (2015) Influence of Operating Variables and Model to Minimize the Use of Anthraquinone in the Soda-Anthraquinone Pulping of Barley Straw. *BioResources*, **10**, 6442-6456. https://doi.org/10.15376/biores.10.4.6442-6456

[12] Mohd Hassan, N.H., Mohammad, N.A., Ibrahim, M., Mohd Yunus, N.Y. and Sarmin, S.N. (2020) Soda-Anthraquinone Pulping Optimization of Oil Palm Empty Fruit Bunch. *BioResources*, **15**, 5012-5031. https://doi.org/10.15376/biores.15.3.5012-5031

[13] Thi, N., *et al*. (2022) Heliyon Cellulose from the Banana Stem : Optimization of Extraction by Response Surface Methodology (RSM) and Charaterization. *Heliyon*, **8**, E11845. https://doi.org/10.1016/j.heliyon.2022.e11845

[14] Orwa, S.A., Mutua, C.A., Kindt, R. and Jamnadass, R. (2009) *Grevillea robusta* A. Cunn. ex R. Br. Proteaceae *Grevillea robusta* A. Cunn. ex R. Br. Database, 1-6.

[15] Wamuragunda, T.W., Kuyah, S., Muthuri, C., Mwangi, P. and Sinclair, F. (2019) Journal of Agriculture, Science and Technology. *Jagst*, **19**, 53-73.

[16] Devaraj, P. and Sugavanam, V. (2006) Monograph on Silver Oak: Grevillea Robusta. International Book Distributors.

[17] Temesgen, A.A. (2021) Modeling and Pulping Variables Optimization of Ethanol-Alkali Pulping and Delignification of Grevillea Robusta in Ethiopia by Response Surface Methodology. *European Journal of Materials Science and Engineering*, **6**, 34-51. https://doi.org/10.36868/ejmse.2021.06.01.034

[18] Israel, A.U., Obot, I.B., Umoren, S.A., Mkpenie, V. and Asuquo, J.E. (2008) Production of Cellulosic Polymers from Agricultural Wastes. *Journal of Chemistry*, **5**, 81-85. https://doi.org/10.1155/2008/436356

[19] Van Soest, P.J., Robertson, J.B. and Lewis, B.A. (1991) Methods for Dietary Fiber, Neutral Detergent Fiber, and Nonstarch Polysaccharides in Relation to Animal Nutrition. *Journal of Dairy Science*, **74**, 3583-3597. https://doi.org/10.3168/jds.S0022-0302(91)78551-2

[20] Javier-Astete, R., Jimenez-Davalos, J. and Zolla, G. (2021) Determination of Hemicellulose, Cellulose, Holocellulose and Lignin Content Using FTIR in *Calycophyllum spruceanum* (Benth.) K. Schum. and *Guazuma crinita* Lam. *PLOS ONE*, **16**, e0256559. https://doi.org/10.1371/journal.pone.0256559

[21] Amal, N., Mohamad, N. and Jai, J. (2022) Heliyon Response Surface Methodology for Optimization of Cellulose Extraction from Banana Stem Using NaOH-EDTA for Pulp and Papermaking. *Heliyon*, **8**, E09114. https://doi.org/10.1016/j.heliyon.2022.e09114

[22] de Almeida, D.P. and Gomide, J.L. (2013) Anthraquinone and Surfactant Effect on Soda Pulping. *O Papel*, **74**, 53-56. https://www.researchgate.net/publication/290975563

[23] L., Y., Ouattara, *et al*. (2022) Optimization of The Autoclave-Assisted Alkaline Delignification of Cocoa (*Theobroma cacao*) Pod Husks Using KOH to Maximize Reducing Sugars. *BioResources*, **17**, 826-848. https://doi.org/10.15376/biores.17.1.826-848

[24] Sarwar Jahan, M., Nashir Uddin, M., Asif Rahman, M., Mostafizur Rahman, M. and Nurul Amin, M. (2016) Soda Pulping of Umbrella Palm Grass (*Cyperus flabettiformic*). *Journal of Bioresources and Bioproducts*, **1**, 85-91. https://doi.org/10.21967/jbb.v1i2.28

[25] Sheltami, R.M., Abdullah, I., Ahmad, I., Dufresne, A. and Kargarzadeh, H. (2012) Extraction of Cellulose Nanocrystals from Mengkuang Leaves (*Pandanus tectorius*), *Carbohydrate Polymers*, **88**, 772-779. https://doi.org/10.1016/j.carbpol.2012.01.062

[26] Diyana, Z.N., Jumaidin, R., Selamat, M.Z., Alamjuri, R.H. and Yusof, F.A.M. (2021) Extraction and Characterization of Natural Cellulosic Fiber from *Pandanus amaryl-*

lifolius Leaves. *Polymers*, **13**, Article 4171. https://doi.org/10.3390/polym13234171

[27] Maheswari, C.U., Muzenda, E., Shukla, M. and Rajulu, A.V. (2016) Extraction and Characterization of Cellulose from Pretreated Ficus (Peepal Tree) Leaf Fibers. *Journal of Natural Fibers*, **13**, 54-64. https://doi.org/10.1080/15440478.2014.984055

[28] Kamaruddin, Z.H., Jumaidin, R., Rushdan, A.I., Selamat, M.Z. and Hanim Alamjuri, R. (2021) Characterization of Natural Cellulosic Fiber Isolated from Malaysian Cymbopogan Citratus Leaves. *BioResources*, **16**, 7729-7750. https://doi.org/10.15376/biores.16.4.7729-7750

[29] Getacho, E. (2022) South African Journal of Chemical Engineering Response Surface Methodology Modeling, Experimental Validation and Optimization of Acid Hydrolysis Process Parameters for Nanocellulose Extraction. *South African Journal of Chemical Engineering*, **40**, 176-185. https://doi.org/10.1016/j.sajce.2022.03.003

[30] Bonface, G.M., Benson, B.G., Urbanus, M., Paul, N., Bilhah, E. and Stephen, O (2020) Optimization of Microalgae Production Conditions Using Genetic Algorithm and Response Surface Methodology. *J. Eng. Agric. Environ.*, **6**, 40-60.

[31] Bozaci, E. and Tağaç, A.A. (2023) Extraction and Characterization of New Cellulosic Fiber from Catalpa Bignonioides Fruits for Potential Use in Sustainable Products. *Polymers*, **15**, Article 201. https://doi.org/10.3390/polym15010201

[32] Morán, J.I., Alvarez, V.A., Cyras, V.P. and Vázquez, A. (2008) Extraction of Cellulose and Preparation of Nanocellulose from Sisal Fibers. *Cellulose*, **15**, 149-159. https://doi.org/10.1007/s10570-007-9145-9

[33] Feleke, K., Thothadri, G., Tufa, H.B., Rajhi, A.A. and Ahmed, G.M.S. (2023) Extraction and Characterization of Fiber and Cellulose from Ethiopian Linseed Straw: Determination of Retting Period and Optimization of Multi-Step Alkaline Peroxide Process. *Polymers*, **15**, Article 469. https://doi.org/10.3390/polym15020469

[34] Owi, W.T., Lin, O.H., Sam, S.T., Chia, C.H., *et al*. (2016) Comparative Study of Microcelluloses Isolated from Two Different Biomasses with Commercial Cellulose. *BioResources*, **11**, 3453-3465. https://doi.org/10.15376/biores.11.2.3453-3465

[35] Romruen, O., Karbowiak, T., Tongdeesoontorn, W., Shiekh, K.A. and Rawdkuen, S. (2022) Extraction and Characterization of Cellulose from Agricultural By-Products of Chiang Rai Province, Thailand. *Polymers*, **14**, Article 1830. https://doi.org/10.3390/polym14091830

[36] Park, S., Baker, J.O., Himmel, M.E., Parilla, P.A. and Johnson, D.K. (2010) Cellulose Crystallinity Index: Measurement Techniques and Their Impact on Interpreting Cellulase Performance. *Biotechnology for Biofuels and Bioproducts*, **3**, Article No. 10. https://doi.org/10.1186/1754-6834-3-10